

## Simulating the focusing of laser-plasma accelerated proton beams

L. Nălbaru<sup>1</sup>, M. Arnold<sup>2</sup>, C. Ticoș<sup>1,3</sup>

<sup>1</sup>*National University of Science and Technology Politehnica Bucharest, Splaiul Independentei no. 313, RO-060042, Bucharest, Romania*

<sup>2</sup>*Institut für Kernphysik, Technische Universität Darmstadt, Schlossgartenstr. 9, 64289 Darmstadt, Germany*

<sup>3</sup>*Extreme Light Infrastructure - Nuclear Physics (ELI-NP), "Horia Hulubei" National Institute for Physics and Nuclear Engineering (IFIN-HH), 30 Reactorului Street, RO-077125 Bucharest-Măgurele, Romania*

### Introduction

Laser-plasma acceleration is a rapidly advancing research field with potential applications in areas such as proton fast ignition [4], warm dense matter studies [5], biomedical research [3] and others. Laser-driven particle beams are generated with a very distinct set of characteristics compared to those resulting from conventional radio-frequency acceleration, making them particularly interesting for the development of compact laser systems for proton beam therapy. The main advantages of laser-plasma accelerated proton beams are the ultra-short pulse duration of the proton bunch (on the order of ps) and the high fluxes ( $10^{11} - 10^{13}$  particles per shot). These characteristics aid in the delivery of ultra-high dose rates, greater than 40 Gy/s, enabling the access to FLASH therapy regime, which reduces toxicity to healthy tissue while still maintaining the therapeutic tumoral response. To fully unlock the potential of employing laser-driven proton beams in clinical applications, other challenges need to be addressed, specifically their broad energy spectrum and large angular divergence.

Here we present a 3D simulation-based study, conducted using COMSOL Multiphysics [6], for the development of a solenoid-based system dedicated to focusing laser-plasma accelerated proton beams for biomedical applications.

### Simulation setup and performance analysis

In this study we examine the influence of different solenoid configurations on the trajectory of a laser-plasma accelerated (LPA) proton beam, with the purpose of focusing it into a millimeter-scale spot. The considered proton beam has an exponentially decaying spectrum, with an energy range from 4 to 20 MeV and a half-angle divergence of up to  $21,25^\circ$ . The particle beam was modeled in accordance with previously reported experimental results involving LPA protons [7]. To achieve our goal, we propose a focusing configuration based on strong magnetic fields generated by a two-solenoid system. The first solenoid has a conical shape, 70 turns, an initial radius of 1.5 cm, a wire radius of 1 mm, an axial pitch of 2.5 mm, and a radial pitch of 0.4 mm. The solenoid was placed with its narrow opening at 1 mm downstream of the source and had a 20 kA current applied to it, generating a peak magnetic field of 9 T. The second solenoid, placed

at a distance of 12 cm from the previous one, has a cylindrical shape, 50 turns, an outer radius of 4 cm, a wire radius of 1 mm and an axial pitch of 2.5 mm. A current of 16 kA was applied to it, resulting in a magnetic field of up to 6 T. Although such high values of the magnetic field could be challenging to achieve in practical experiments, the proposed solution remains valid in the context of magnetic fields that are steady for periods of time as short as the proton beam's transit time through the focusing system, which would be on the order of a few nanoseconds. Pulsed coil systems capable of generating high magnetic fields for such short durations have previously been reported [8, 9]. Figure 1 shows the spatial distribution of the magnetic field generated by the two-solenoid system in the  $yz$  plane, as resulted from the COMSOL simulations.

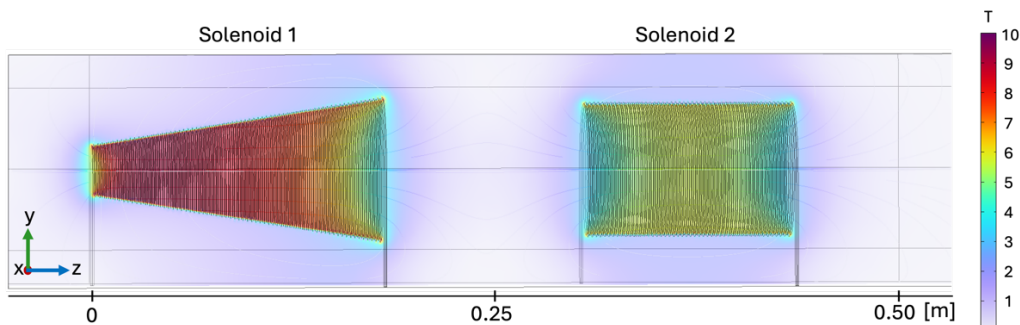


Fig. 1. Spatial distribution of the magnetic field generated by the two-solenoid focusing configuration for current values of 20 kA applied to the first solenoid and 16 kA to the second one.

The performance of the focusing system was analyzed in respect to the previously described proton beam emitted from a  $2 \mu\text{m}$  radius spot along the  $z$ -axis. Due to the direct proportionality between the focal length of a solenoid and the momentum of the particles, lower-energy protons experience stronger focusing effects, reaching their focus spot before exiting the second solenoid. As the proton energy increases, the influence of the magnetic field on their trajectory decreases; thus, higher-energy protons are initially collimated by the first solenoid and focused after passing through the second one. Figure 2 (a) and (b) presents the trajectories of 6 to 8 MeV protons passing through the focusing system, showing this distinct behavior between lower-energy particles, which are focused within the second solenoid, Figure 2 (a), and higher-energy protons, which are focused only after completely passing through both magnetic elements, Figure 2 (b).

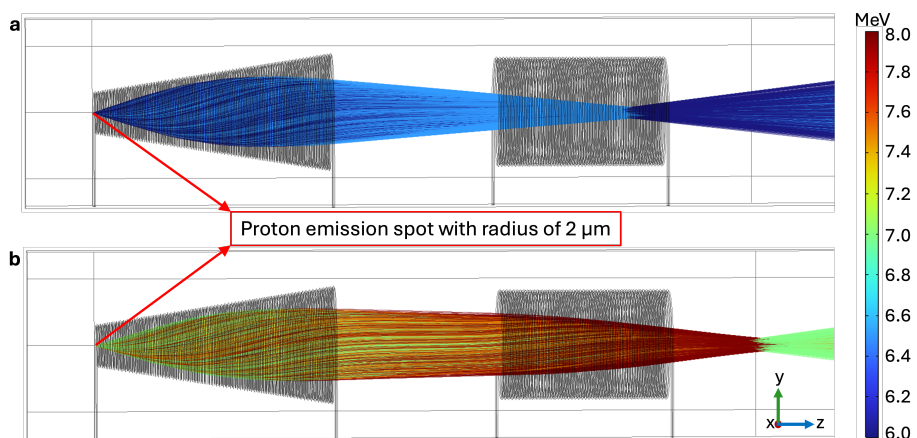


Fig. 2. 2D projection on  $yz$ -plane of the proton trajectories after passing through the two-solenoid focusing configuration represented for energies of: a) 6 and 6.5 MeV and b) 7, 7.5 and 8 MeV.

The system's performance was analyzed in terms of focus spot size and position, as well as capturing efficiencies, considering all particles with energies high enough to allow exiting the two-solenoid system before being focused. The focus spot position, measured in respect to the source, ranges from 0.5 m to 1.9 m for protons with energies between 8 and 20 MeV. The radius of the focus spot was also measured, resulting in values between 4 and 15 mm. Protons in the energy range from 16 to 20 MeV presented the highest values for both focus spot position and size. To further decrease the values of these parameters, we added 20 additional turns to the second solenoid, extending the entire setup by 5 cm and increasing the spatial distribution of the magnetic field responsible with the focusing of higher-energy protons. Thus, an optimized version of the two-solenoid system was implemented. A comparative performance analysis between the initial configuration and the modified version is illustrated in Figure 3 for 5 specific energy intervals ranging from 8 to 20 MeV. The first plot shows the radius of the focus spot, while the second one illustrates its position on the propagation axis measured in respect to the source. An overall decrease in focus spot size was obtained with the optimized version over all energy intervals, with the highest drop in value of 10.5 mm corresponding to 16 to 20 MeV protons. The 20 additional turns added to the second coil also decreased the focus spot position, as resulted from the two data sets represented in Figure 3 (b). The difference in performance between the two configurations becomes more pronounced with increasing particle energy, resulting in a decrease of almost 1 m of the focus spot position for the higher energy protons. In terms of collection efficiency, a comparison between the initial and optimized setups shows a clear improvement in proton capturing performance across all energy intervals. In the initial configuration, efficiency ranged from 86% to 99%, with noticeable drops for mid-energy protons. In contrast, the optimized setup achieved near-complete capture across the spectrum, reaching 100% efficiency for protons between 8 and 11 MeV, and over 92% for mid-to-high-energy protons.

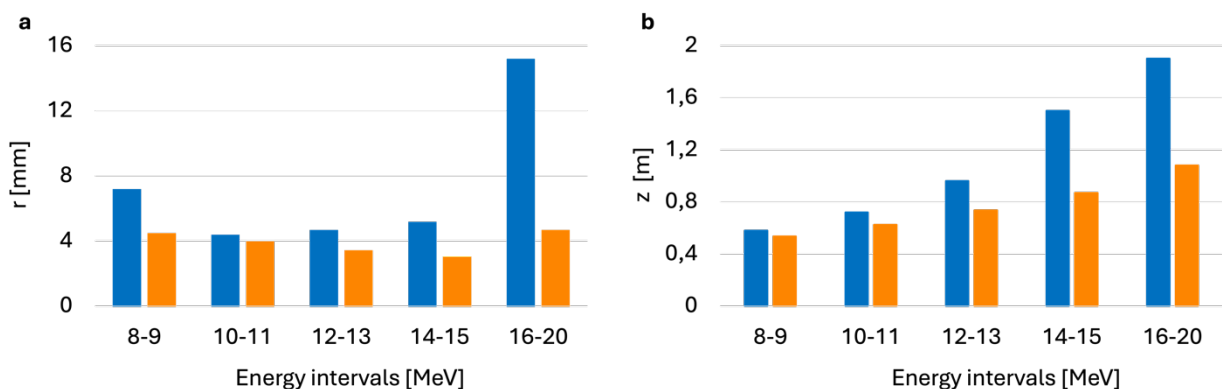


Fig. 3. Comparative analysis between the performance of the initial focusing configuration (illustrated with blue) and the optimised version (illustrated with orange), across specific energy intervals, evaluating: a) the radius of the focus spot and b) its position on the propagation axis.

A dose monitoring study was also included in the simulation. For this, we added a cylindrical target volume of 4 mm length and 5 mm diameter, with water composition to closely replicate the soft tissue interaction with radiation. For the irradiation of the sample, the proton beam spectrum

was narrowed down to the 16 to 20 MeV energy range, with the source emitting a total number of  $1.18 \cdot 10^6$  protons. A decrease in statistics by a few orders of magnitude, compared to literature reported results in LPA beams, was imposed by the high computational demands associated with the dose monitoring simulations. The modeled sample was placed at  $z = 1.08$  m, the focus spot position for the energy range of interest. This way, we tested for the irradiation of a volume resembling a superficial tumor, using a focused laser-plasma accelerated proton beam with energies between 16 and 20 MeV. After irradiation, the cylindrical target volume received a total absorbed dose of 25 mGy. Taking into account the pulse duration of the proton bunch, a dose rate of  $1.2 \cdot 10^7$  Gy/s was obtained, reaching the FLASH therapy regime.

## Conclusions

The here described 3D COMSOL simulation-based study investigates the performance of a two-solenoid configuration dedicated to focusing a laser-plasma accelerated proton beam, with an energy range from 4 to 20 MeV and a divergence of up to  $21^\circ$ , with the aim of future development of biomedical applications in proton beam therapy. Two high-current dual-solenoid configurations, consisting of both conical and cylindrical coils, were tested and compared in terms of focus spot size and position. The optimized setup presented capturing efficiencies of over 92%, being able to obtain focus spots of millimetric ranges at distances of up to 1 m from the source. A dose monitoring simulation study upon a cylindrical target volume, employing 16 to 20 MeV protons, was implemented, resulting in dose rates specific to the FLASH therapy regime.

## Acknowledgment

This work is supported by the Deutsche Forschungsgemeinschaft (DFG, German Research Foundation) – Project-ID 499256822 – GRK 2891 ‘Nuclear Photonics’ and by Project ELI-RO/DFG/2023\_001 ARNPhot funded by the Institute of Atomic Physics, Romania.

## References

- [1] F. Romano, et al., NIM-A 829, 153 (2016).
- [2] F. Kroll, et al., Nat. Phys. 18, 316–322 (2022).
- [3] M. Wu, et al., NIM-A 955, 163249 (2020).
- [4] M. Borghesi, et al., Fusion Sci. and Technol. 49, 412 (2006).
- [5] M. Roth, et.al., Plasma Physics and Controlled Fusion 51, 124039 (2009).
- [6] COMSOL Inc., Multiphysics (2020).
- [7] F. Nuernberg, et al., Rev. Sci. Instrum. 80, 10.1063/1.3086424 (2009).
- [8] G. Fiksel, et al., Rev. Sci. Instrum. 86, 016105 (2015).
- [9] D. Rovang, et al., Rev. Sci. Instrum. 85, 124701 (2014).